

QED calculations of intra- L -shell singly excited states in Be-like ions

A. V. Malyshev,^{1,2} Y. S. Kozhedub,¹ V. M. Shabaev,^{1,2} and I. I. Tupitsyn¹

¹*Department of Physics, St. Petersburg State University, Universitetskaya 7-9, 199034 St. Petersburg, Russia*

²*Petersburg Nuclear Physics Institute named by B.P. Konstantinov of National Research Center “Kurchatov Institute”, Orlova roscha 1, 188300 Gatchina, Leningrad region, Russia*

The *ab initio* approach is used to evaluate the excitation energies of the $2s2p^{2S+1}P_J$ states from the ground state as well as the $2s2p^3P_1 \rightarrow 2s2p^3P_0$ and $2s2p^3P_2 \rightarrow 2s2p^3P_1$ transition energies for selected Be-like highly-charged ions over a wide range: from Ar^{14+} to U^{88+} . The issue of a strong level mixing due to the proximity of states with the same symmetry is addressed by applying the QED perturbation theory for quasidegenerate levels. The employed approach combines a rigorous perturbative QED treatment up to the second order with electron-electron correlation contributions of the third and higher orders calculated in the Breit approximation. The higher-order QED effects are estimated using the model-QED-operator approach. The nuclear-recoil and nuclear-polarization effects are taken into account as well. The performed calculations are accompanied with a thorough analysis of uncertainties due to uncalculated effects. The most accurate theoretical predictions for the excitation and transition energies in Be-like ions are obtained, which, in general, are in perfect agreement with the available experimental data.

I. INTRODUCTION

Quantum electrodynamics (QED) is widely recognized as a powerful tool for describing the electronic structure and various properties of bound systems composed of electrically charged particles. The strengths of this theory are clearly manifested in the study of highly-charged ions (HCIs) [1]. In HCIs, non-trivial QED effects are significantly enhanced compared to those in light atoms. On the other hand, these effects are not masked by an uncertainty with which electron-electron correlation effects can be treated, as is usually the case for neutral systems. All this makes HCIs ideal candidates for a diverse range of fundamental investigations. For example, high-precision measurements with HCIs traditionally form the basis for comprehensive tests of bound-state-QED methods [2–10]. Furthermore, HCIs can also be used for the precise determination of fundamental constants [11–14], in the search for their possible variation [15–17], and in numerous other applications [18, 19].

To date, one of the most rigorous tests for bound-state-QED methods is associated with the measurement of the $2p_{1/2} \rightarrow 2s$ transition in Li-like uranium [20–22], for related theory see, e.g., Refs. [23, 24]. In our recent work [25], which was primarily devoted to QED calculations for Xe^{50+} , we also evaluated the $2p_{1/2} \rightarrow 2s$ transition in Be-like uranium. The theoretical accuracy achieved was found to be comparable to that for Li-like uranium. As the measurements of these systems can also be performed at a comparable level of accuracy [22], both these charge states become equally attractive for probing bound-state QED in the strong-coupling regime. A similar conclusion was reached in Ref. [26], where the $2p_{3/2} \rightarrow 2s$ transition energies in He-, Li-, and Be-like uranium, as well as all their pairwise differences, were calculated. The results reported in Ref. [26] demonstrate good agreement with the high-precision measurements, accomplished recently at the

ESR storage ring at the GSI in Darmstadt [27].

At the same time, bound-state-QED calculations of Be-like ions are in certain respects more challenging than those of Li-like ions. In Be-like ions, the proximity of energy levels with the same symmetry results in their strong mixing by the electron-electron interaction. As a consequence, the conventional single-level QED perturbative approach, which appears to be valid for Li-like ions [23, 24], may prove inadequate when applied to Be-like ions [25]. This strong mixing of energy levels inevitably arises, e.g., in the study of the $2s2s^1S_0$ ground state of Be-like ions [28, 29] (for the sake of brevity, we do not include the closed K shell into the state designations). The intra- L -shell singly excited states with the total angular momentum $J = 1$ are also significantly mixed by the electron-electron interaction.

The investigation of the electronic structure of Be-like HCIs has been addressed many times previously by means of a variety of relativistic approaches [28, 30–54]. However, to the best of our knowledge, all these calculations treated the QED effects at best within some one-electron (first-order) approximations only, demonstrating a significant scatter of the resulting theoretical predictions. In contrast, the method developed by us in Ref. [25] takes into account all the relevant QED contributions up to the second order, overcoming the challenges due to the level mixing by using perturbation theory (PT) for quasidegenerate levels. The first implementation of this method for Be-like HCIs was realized in Refs. [25, 26, 55] for the ground and low-lying excited states in xenon ion, as well as for selected transitions in molybdenum and uranium ions. The present work extends these calculations to a broader range of Be-like HCIs: from argon to uranium. Namely, we evaluate the excitation energies of the $2s2p^3P_{0,1,2}$ and $2s2p^1P_1$ states from the $2s2s^1S_0$ ground state. The $2s2p^3P_1 \rightarrow 2s2p^3P_0$ and $2s2p^3P_2 \rightarrow 2s2p^3P_1$ transition energies are also considered. In all of the cases, particular attention is paid to a comprehensive examination of the uncertainties associated with uncalculated

effects. The obtained theoretical predictions are compared with the available experimental data [56–70] and the results of the previous calculations. In general, good agreement is found with the former.

II. THEORETICAL APPROACH AND COMPUTATIONAL DETAILS

In this section, we briefly describe the *ab initio* method employed in the present work to evaluate the electronic structure of Be-like HCIs. Some numerical aspects of the calculations are discussed here as well. For further details, the reader is referred to Refs. [25, 26, 55] and references therein.

We use PT which is constructed in the Furry picture of QED [71] according to the two-time Green’s function (TTGF) method [72]. To zeroth order, this means that individual electrons obey the Dirac equation with some local spherically symmetric binding potential V . To better keep under control the accuracy of the calculations and to analyze the convergence of the perturbation series, we perform all calculations for several choices of V . First, we take V to be the Coulomb potential of an extended nucleus, $V = V_{\text{nuc}}$. Second, we modify V by adding some screening potential to the nuclear one, $V = V_{\text{nuc}} + V_{\text{scr}}$. The latter is introduced to partially take into account the interelectronic-interaction effects from the very beginning. Obviously, this modification leads to a rearrangement of perturbation series, since the counterterm $\delta V = -V_{\text{scr}}$ is to be treated perturbatively. As in Ref. [25], we use two variants for the screening potential: (i) the core-Hartree (CH) potential generated by the closed K shell; and (ii) the local Dirac-Fock (LDF) potential [73].

As noted in Sec. I, for a proper description of the electronic structure of Be-like HCIs, it is crucial to take into account the proximity of energy levels possessing the same symmetry. Within the TTGF method this issue is solved by applying the QED PT for quasidegenerate levels [72]. The close-lying levels are grouped into a finite-dimensional model subspace Ω , and an effective Hamiltonian H_{eff} , acting in this subspace, is constructed step-by-step including all relevant contributions. The energies of the states under consideration are obtained by diagonalizing the matrix of H_{eff} . In this respect, the standard QED PT for a single level can be considered as a special case with the one-dimensional Ω . It is important to note a peculiarity of PT with the dimension of the model subspace greater than one: the contributions due to different effects are not strictly additive, as they are mixed during the diagonalization. Therefore, this diagonalization must be performed at the last stage of the calculations.

Before proceeding with the discussion of the model subspaces used in the present work, let us comment on the notations. Our *ab initio* method represents the fully relativistic approach. All the unperturbed many-electron wave functions are constructed in the jj cou-

pling from Slater determinants, which are in turn built from the solutions of the one-electron Dirac equation. However, to emphasize the impact of energy-level mixing, the LS -coupling notation is utilized to refer to the states resulting from the H_{eff} -matrix diagonalization procedure. For the sake of uniformity, we apply this also to the states obtained using one-dimensional model subspaces. More specifically, the $(2s2p_{1/2})_0$ and $(2s2p_{3/2})_2$ levels turn out to be separated from other levels of the same symmetry. Therefore, their energies are calculated using PT for a single level. The corresponding states are designated with $2s2p^3P_0$ and $2s2p^3P_2$, respectively. The $(2s2p_{1/2})_1$ and $(2s2p_{3/2})_1$ levels exhibit strong mixing with each other. We employ the two-dimensional model subspace Ω spanned by these levels. The resulting states are referred to as $2s2p^3P_1$ and $2s2p^1P_1$. The influence of level mixing on the QED effects can be identified by recalculating the energies of the $(2s2p_{1/2})_1$ and $(2s2p_{3/2})_1$ levels regarding them as the single ones. In the present paper, the energies of the intra- L -shell singly excited states are given relative to the $2s2s^1S_0$ ground state. Therefore, an accurate description of the latter is a vital task too. As in Refs. [25, 55], we use the three-dimensional model subspace spanned by the $(2s2s)_0$, $(2p_{1/2}2p_{1/2})_0$, and $(2p_{3/2}2p_{3/2})_0$ levels. In addition, we study the two-dimensional Ω spanned by only the first two of these levels and the one-dimensional Ω corresponding to the $(2s2s)_0$ level. By combining the results of these three distinct calculations for the ground state, we gain a deeper understanding of the strong interplay between the electron-electron correlation and QED effects, which was noted in Ref. [25].

The developed approach rigorously treats all contributions up to the second order of the QED PT. The computational expressions are derived within the TTGF method in the formalism, in which the closed K shell is assigned to the vacuum [72]. In this formalism, only two L -shell electrons remain, and, therefore, the problem is reduced to the consideration of one- and two-electron Feynman diagrams. The necessary diagrams, except for the one-electron two-loop diagrams and the counterterm diagrams, which arise when V_{scr} is included into the zeroth-order Hamiltonian, are shown in Fig. 1. The derivation of the formulas is performed for an arbitrary size of the model subspace Ω . By passing to the standard QED vacuum, we explicitly extract from the obtained formulas the contributions describing the interaction with the K -shell electrons. The calculations are organized as described in Ref. [26]: (i) the one-electron two-loop QED corrections are obtained using the results of Refs. [74, 75]; and (ii) all other contributions are rigorously evaluated for the three binding potentials V listed above. Further details of the QED calculations can be found in our previous works, see, e.g., Refs. [25, 26, 55, 76–79].

The higher-order interelectronic-interaction effects are treated within the Breit approximation based on the Dirac-Coulomb-Breit (DCB) Hamiltonian. There are a variety of well-established methods for solving the DCB

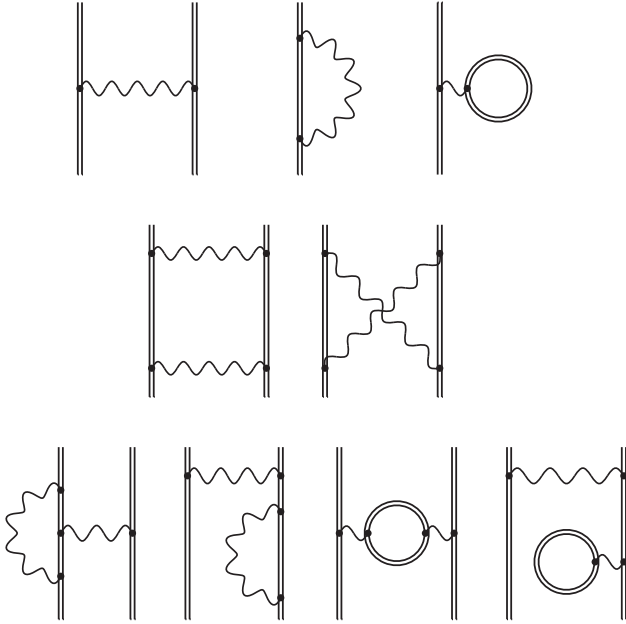


FIG. 1. First- and second-order Feynman diagrams, except for the one-electron two-loop diagrams. The counterterm diagrams are not shown. The double line corresponds to the electron propagator in the binding potential V . The formalism, in which the $1s$ state is assigned to the vacuum, is used [72]. The wavy line represents the photon propagator.

equation. In our approach, we use the configuration-interaction (CI) method in the basis of the Dirac-Sturm orbitals [80, 81]. The key point is to accurately merge the results of QED and electron-electron correlation effects. While this issue is relatively straightforward in the case of PT for a single level [77, 82], it becomes more complex when considering PT for quasidegenerate levels. For this aim, we utilize the procedure initially proposed in Ref. [79] and described in details in Refs. [55, 78].

To complete the brief description of the method, it should be noted that the corrections arising from the nuclear-recoil [83–89] and nuclear-polarization [74, 90, 91] effects are also taken into account. In addition, we employ the model-QED operator [92, 93] to estimate the higher-order screened QED contributions, which correspond to the Feynman diagrams similar to those in the last line in Fig. 1 but with an additional photon line mediating the electron-electron interaction. The details of all these calculations are summarized in Ref. [26].

The calculations are performed for the following Be-like HCIs: argon $^{40}\text{Ar}^{14+}$, krypton $^{84}\text{Kr}^{32+}$, molybdenum $^{98}\text{Mo}^{38+}$, xenon $^{132}\text{Xe}^{50+}$, lead $^{208}\text{Pb}^{78+}$, bismuth $^{209}\text{Bi}^{79+}$, thorium $^{232}\text{Th}^{86+}$, and uranium $^{238}\text{U}^{88+}$. The nuclear masses and root-mean-square radii are assumed to be the same as in Ref. [74]. The nuclear-charge distribution is described by the Fermi model with the thickness parameter set to 2.3 fm. For uranium, we also consider the correction caused by

the nuclear-deformation effect [23]. The hyperfine structure due to the nuclear-magnetic moment of ^{209}Bi is neglected. The values of the fundamental constants from Ref. [94] are employed throughout the calculations.

III. NUMERICAL RESULTS AND DISCUSSIONS

In this section, we present the results of our QED calculations for Be-like HCIs. First, we demonstrate the level mixing using the results of the CI method. Second, we provide an error budget and estimate the uncertainties associated with the uncalculated higher-order contributions. Finally, we present our theoretical predictions for the $2s2s^1S_0 \rightarrow 2s2p^3P_{0,1,2}$ and $2s2s^1S_0 \rightarrow 2s2p^1P_1$ excitation energies and for the $2s2p^3P_1 \rightarrow 2s2p^3P_0$ and $2s2p^3P_2 \rightarrow 2s2p^3P_1$ transition energies. These predictions are compared with available experimental data and results of previous relativistic calculations.

Since the CI method is a non-perturbative approach with respect to the interelectronic interaction, the level mixing does not pose a problem in its framework. In our implementation of the CI method, the DCB operator acts in a space of Slater determinants constructed from the positive-energy eigenfunctions of the Dirac Hamiltonian. The latter includes the same local binding potential as that which determines the QED PT. In principle, other one-electron operators, e.g., the nonlocal Dirac-Fock one, can be used to determine a decomposition into the positive- and negative-energy spectra. There is an ambiguity in this matter within the Breit approximation [95]. We use the variant specified above, since it follows naturally from QED [10, 96] and thus provides the most accurate merging with the QED calculations. Nevertheless, the ambiguity of the Breit-approximation results associated with the choice of the local binding potential still remains, and it can be resolved only within the rigorous QED approach, see the related discussions in Refs. [26, 78].

In Table I, an example of our CI calculations of Be-like HCIs is presented. Within the CI method, the many-electron wave functions are sought in the form of an expansion in configuration-state functions (CSFs) with the given values of the total angular momentum J and its projection M_J . Table I shows the coefficients for the CSFs assigned to the model subspaces described above. Namely, the coefficients A_1 , A_2 , and A_3 correspond to the $(2s2s)_0$, $(2p_{1/2}2p_{1/2})_0$, and $(2p_{3/2}2p_{3/2})_0$ levels contributing to the ground state. The coefficients B_1 and B_2 correspond to the $(2s2p_{1/2})_1$ and $(2s2p_{3/2})_1$ levels in the $2s2p^3P_1$ state, while the coefficients C_1 and C_2 have the same meaning for the $2s2p^1P_1$ state. The values of the coefficients presented in Table I are not to be regarded as the exact or final ones. They are obtained for a certain finite size of configuration space, prior to any extrapolation to the infinite-dimensional space, and serve only to illustrate the level mixing. Moreover, the

TABLE II: Error budget (*continued*).

Source	$2s2p^3P_0$ $-2s2s^1S_0$	$2s2p^3P_1$ $-2s2s^1S_0$	$2s2p^3P_2$ $-2s2s^1S_0$	$2s2p^1P_1$ $-2s2s^1S_0$	$2s2p^3P_1$ $-2s2p^3P_0$	$2s2p^3P_2$ $-2s2p^3P_1$
H.o. QED, scatter	0.00094	0.00086	0.00028	0.00094	0.00008	0.00058
Other	0.00030	0.00033	0.00030	0.00041	0.00030	0.00030
Total	0.0021	0.0020	0.0019	0.0021	0.0018	0.0019
$Z = 42$						
1el FNS	0.00011	0.00011	0.00011	0.00011	< 0.00001	< 0.00001
1el nucl. pol.	0.00010	0.00010	0.00010	0.00010	< 0.00001	< 0.00001
1el 2loop	0.00061	0.00061	0.00063	0.00063	< 0.00001	0.00028
H.o. QED, ≥ 3 ph	0.0022	0.0022	0.0022	0.0022	0.0022	0.0022
H.o. QED, 2loop	0.0018	0.0018	0.0018	0.0018	0.0018	0.0018
H.o. QED, scatter	0.0012	0.0012	0.00007	0.00069	0.00007	0.0013
Other	0.00043	0.00046	0.00043	0.00050	0.00042	0.00042
Total	0.0032	0.0032	0.0029	0.0030	0.0029	0.0031
$Z = 54$						
1el FNS	0.00097	0.00097	0.00097	0.00097	< 0.00001	0.00003
1el nucl. pol.	0.00047	0.00047	0.00047	0.00047	< 0.00001	0.00001
1el 2loop	0.0027	0.0027	0.0028	0.0028	< 0.00001	0.0012
H.o. QED, ≥ 3 ph	0.0044	0.0044	0.0044	0.0044	0.0044	0.0044
H.o. QED, 2loop	0.0043	0.0043	0.0043	0.0043	0.0043	0.0043
H.o. QED, scatter	0.0026	0.0024	0.0012	0.00030	0.00030	0.0037
Other	0.00082	0.00083	0.00080	0.00086	0.00080	0.00078
Total	0.0074	0.0073	0.0070	0.0069	0.0063	0.0073
$Z = 82$						
1el FNS	0.022	0.022	0.022	0.022	< 0.0001	0.0017
1el nucl. pol.	0.0025	0.0025	0.0025	0.0025	< 0.0001	0.0002
1el 2loop	0.038	0.038	0.037	0.037	< 0.0001	0.0090
H.o. QED, ≥ 3 ph	0.017	0.017	0.017	0.017	0.017	0.017
H.o. QED, 2loop	0.019	0.019	0.019	0.019	0.019	0.019
H.o. QED, scatter	0.015	0.013	0.0084	0.0056	0.0025	0.021
Other	0.0036	0.0036	0.0035	0.0036	0.0031	0.0032
Total	0.053	0.052	0.051	0.051	0.026	0.035
$Z = 83$						
1el FNS	0.026	0.026	0.026	0.026	< 0.0001	0.0021
1el nucl. pol.	0.013	0.013	0.013	0.013	< 0.0001	0.0012
1el 2loop	0.041	0.041	0.040	0.040	< 0.0001	0.0074
H.o. QED, ≥ 3 ph	0.018	0.018	0.018	0.018	0.018	0.018
H.o. QED, 2loop	0.020	0.020	0.020	0.020	0.020	0.020
H.o. QED, scatter	0.016	0.013	0.0087	0.0059	0.0027	0.022
Other	0.0042	0.0042	0.0042	0.0042	0.0037	0.0038
Total	0.059	0.058	0.057	0.057	0.027	0.036
$Z = 90$						
1el FNS	0.11	0.11	0.11	0.11	< 0.0001	0.011
1el nucl. pol.	0.012	0.012	0.012	0.012	< 0.0001	0.0012
1el 2loop	0.074	0.074	0.073	0.073	< 0.0001	0.015
H.o. QED, ≥ 3 ph	0.025	0.025	0.025	0.025	0.025	0.025
H.o. QED, 2loop	0.027	0.027	0.027	0.027	0.027	0.027
H.o. QED, scatter	0.024	0.020	0.011	0.008	0.0040	0.031

TABLE II: Error budget (*continued*).

Source	$2s2p^3P_0$	$2s2p^3P_1$	$2s2p^3P_2$	$2s2p^1P_1$	$2s2p^3P_1$	$2s2p^3P_2$
	$-2s2s^1S_0$	$-2s2s^1S_0$	$-2s2s^1S_0$	$-2s2s^1S_0$	$-2s2p^3P_0$	$-2s2p^3P_1$
Other	0.010	0.010	0.009	0.009	0.0055	0.0062
Total	0.14	0.14	0.13	0.13	0.037	0.052
$Z = 92$						
1el FNS	0.034	0.034	0.034	0.034	< 0.0001	0.0040
1el nucl. pol.	0.020	0.020	0.020	0.020	< 0.0001	0.0022
1el 2loop	0.088	0.088	0.086	0.086	< 0.0001	0.018
H.o. QED, ≥ 3 ph	0.027	0.027	0.027	0.027	0.027	0.027
H.o. QED, 2loop	0.030	0.030	0.030	0.030	0.030	0.030
H.o. QED, scatter	0.026	0.022	0.012	0.008	0.0043	0.034
Other	0.009	0.009	0.009	0.009	0.0068	0.0071
Total	0.11	0.11	0.10	0.10	0.041	0.056

An essential part of the present study consists in a thorough analysis of the uncertainties that have to be ascribed to the theoretical predictions obtained. The error budget of our calculations is summarized in Table II. The undertaken analysis of the uncertainties follows, with minor modifications, the scheme described in detail in Refs. [25, 26]. For the sake of self-sufficiency, let us briefly discuss this issue here.

In Table II, the first line “1el FNS” presents the uncertainties caused by the finite-nuclear-size (FNS) effect on the one-electron Dirac energies. For uranium, these uncertainties are obtained within the evaluation of the nuclear-deformation correction [23]. For other ions, they are estimated by quadratically summing the variation due to changing the root-mean-square radius within its error bars and the variation due to replacing the Fermi model of the nuclear-charge distribution by a homogeneously-charged-sphere one. The second line “1el nucl. pol.” shows the uncertainties associated with the nuclear-polarization effect. They are estimated according to a prescription formulated in Ref. [74] for H-like ions. The third line “1el 2loop” gives the uncertainties of the one-electron two-loop contributions. They are also taken from Ref. [74]. Because of the level mixing, these one-electron uncertainties do not vanish even for the $2s2p^3P_1 \rightarrow 2s2p^3P_0$ transition energy. The three subsequent lines in Table II provide the results of our various estimations of the uncalculated higher-order QED effects. First, in the line “H.o. QED, ≥ 3 ph”, we estimate the QED correction to the interelectronic-interaction contribution related to the exchange by three or more photons. For all the excitation and transition energies, we assign the same value of this uncertainty according to the procedure from Ref. [78]. Namely, the third- and higher-order Breit-approximation value obtained within the CI method is multiplied by the doubled ratio of the corresponding second-order QED correction and its Breit-approximation counterpart. The ground-state binding energy evaluated for the LDF potential is used for this purpose. The calculations show

that for other states the procedure gives values of the same order of magnitude. Second, in the line “H.o. QED, 2loop”, we estimate the screening of the one-electron two-loop contribution by multiplying the corresponding term for the $1s$ state by a conservative factor of $2/Z$. Third, in the line “H.o. QED, scatter”, we estimate the convergence of the perturbation series by analyzing the scatter of the results obtained for different binding potentials V . We take the absolute value of the difference between the total results for the LDF and CH potentials and add to it the absolute value of the correction obtained for the LDF potential using the model-QED-operator approach. The line labeled “Other” summarizes all other sources of the uncertainties: (i) numerical errors of the QED and CI calculations, which are estimated by analyzing the convergence of the results with respect to the partial-wave expansions and the sizes of the finite-basis sets used; (ii) uncertainties due to the remaining part of the FNS effect, including that for the nuclear recoil contribution [99–102]; (iii) an estimate of the QED part of the nuclear recoil effect beyond the independent-electron approximation; and (iv) a similar estimate for the nuclear-polarization effect. The latter two estimates are obtained by multiplying the corresponding one-electron contributions for the $1s$ state by a factor of $2/Z$. The consideration of this additional uncertainty for the nuclear-polarization effect compared to the one given in the row “1el nucl. pol.” is obviously meaningless for the $2s2s^1S_0 \rightarrow 2s2p^3P_{0,1,2}$ and $2s2s^1S_0 \rightarrow 2s2p^1P_1$ excitation energies. However, this has sense for the $2s2p^3P_1 \rightarrow 2s2p^3P_0$ and $2s2p^3P_2 \rightarrow 2s2p^3P_1$ transition energies. The total uncertainties are evaluated by quadratically summing all the errors listed above. The convergence of the perturbation series and the overall performance of the numerical methods are kept under control by carrying out the calculations for the Coulomb, CH, and LDF potentials. For the same purposes, the calculations are performed in both Feynman and Coulomb gauge for the photons mediating the interelectronic interaction, see the related

discussion, e.g., in Ref. [26]. An example of how perturbation series starting from different initial approximations converge can be found in Refs. [26, 77].

In order to better represent the competing sources of theoretical uncertainty, the individual contributions in Table II are given with extra significant digits. To emphasize that some source provides a small but nonzero value, we indicate an inequality, such as “ < 0.000001 ”. From Table II, it can be seen that for low- Z Be-like HCIs the total uncertainties arise mainly from the uncalcu-

lated higher-order QED effects. For the $2s2p^3P_1 \rightarrow 2s2p^3P_0$ and $2s2p^3P_2 \rightarrow 2s2p^3P_1$ transition energies, this holds true also for high- Z ions. However, for the $2s2s^1S_0 \rightarrow 2s2p^3P_{0,1,2}$ and $2s2s^1S_0 \rightarrow 2s2p^1P_1$ excitation energies in heavy Be-like HCIs, the situation currently differs. In this case, the total theoretical uncertainties are determined by the calculations of the one-electron two-loop contribution. The uncertainties due to the FNS and nuclear-polarization effects also come into play.

TABLE III: The excitation energies of the $2s2p^3P_{0,1,2}$ and $2s2p^1P_1$ states from the $2s2s^1S_0$ ground state in Be-like ions (in eV). The theoretical (Th.) results are compared with the experimental (Expt.) values.

$2s2p^3P_0$ $-2s2s^1S_0$	$2s2p^3P_1$ $-2s2s^1S_0$	$2s2p^3P_2$ $-2s2s^1S_0$	$2s2p^1P_1$ $-2s2s^1S_0$	Th./Expt.	Year	Reference
$Z = 18$						
28.35403(41)	29.24427(59)	31.32954(39)	56.06799(70)	Th.	2024	This work
28.354(95)	29.244(95)	31.331(95)	56.069(95)	Th.	2019	Kaygorodov <i>et al.</i> [54]
28.3489	29.2451	31.3201		Th.	2017	Li <i>et al.</i> [53]
28.360(12)	29.248(16)	31.334(12)	56.085(29)	Th.	2015	Yerokhin <i>et al.</i> [50]
28.3673	29.2585	31.3451	56.0268	Th.	2005	Gu [43]
	29.243	31.330	55.990	Th.	2000	Safronova [39]
		31.3293		Th.	2000	Majumder and Das [40]
28.3489	29.2397	31.3268	55.9872	Th.	1996	Safronova <i>et al.</i> [35]
28.3520	29.2433	31.3287	56.0671	Th. [†]	1983	Edlén [31]
28.3532(48)	29.2429(20)	31.3283(20)	56.0634(81)	Expt. [‡]	2010	Saloman [69]
	29.243(2)		56.071(8)	Expt.	1978	Dere [57]
	29.241(2)		56.063(8)	Expt.	1975	Widing [56]
$Z = 36$						
62.6306(21)	72.9862(20)	125.6572(19)	170.4200(21)	Th.	2024	This work
62.64(73)	72.98(73)	125.69(73)	170.45(73)	Th.	2019	Kaygorodov <i>et al.</i> [54]
62.6228	72.9867	125.656	170.454	Th.	2008	Cheng <i>et al.</i> [46]
62.6970	73.0647	125.7730	170.5499	Th.	2005	Gu [43]
	72.975	125.639	170.397	Th.	2000	Safronova [39]
62.6198	72.9751	125.6409	170.3990	Th.	1996	Safronova <i>et al.</i> [35]
62.5216	72.8834	125.6282	170.6618	Th. [†]	1983	Edlén [31]
62.67(12)				Expt.	1991	Sugar and Musgrove [61]
	72.998(11)	125.651(16)	170.411(47)	Expt.	1989	Denne <i>et al.</i> [58]
$Z = 42$						
75.2876(32)	90.0049(32)	197.9864(29)	248.4990(30)	Th.	2024	This work
75.3(12)	90.0(12)	198.0(12)	248.5(12)	Th.	2019	Kaygorodov <i>et al.</i> [54]
75.2724	90.0053	197.982	248.540	Th.	2008	Cheng <i>et al.</i> [46]
75.3798	90.1169	198.1860	248.7330	Th.	2005	Gu [43]
	89.981	197.94	248.47	Th.	2000	Safronova [39]
	90.0061		248.5428	Th.	1997	Chen and Cheng [36]
75.2691	89.9895	197.9554	248.4831	Th.	1996	Safronova <i>et al.</i> [35]
	89.982(37)		248.523(33)	Th.	1992	Lindroth and Hvarfner [32]
	89.983(20)		248.45(15)	Expt.	1989	Denne <i>et al.</i> [59]
$Z = 54$						
104.5305(74)	127.2997(73)	469.4832(70)	532.8009(69)	Th.	2024	This work
104.5(25)	127.3(25)	469.6(25)	532.9(25)	Th.	2019	Kaygorodov <i>et al.</i> [54]

TABLE III: Excitation energies (*continued*).

$2s2p^3P_0$ $-2s2s^1S_0$	$2s2p^3P_1$ $-2s2s^1S_0$	$2s2p^3P_2$ $-2s2s^1S_0$	$2s2p^1P_1$ $-2s2s^1S_0$	Th./Expt.	Year	Reference
104.475	127.282	469.449	532.877	Th.	2008	Cheng <i>et al.</i> [46]
104.663	127.475	470.004	533.401	Th.	2005	Gu [43]
	127.168	469.25	532.62	Th.	2000	Safronova [39]
	127.301		532.854	Th.	1997	Chen and Cheng [36]
104.482	127.267	469.386	532.759	Th.	1996	Safronova <i>et al.</i> [35]
	127.269(46)	469.474(81)	532.801(16)	Expt.	2015	Bernhardt <i>et al.</i> [70]
	127.260(26)			Expt.	2005	Feili <i>et al.</i> [67]
	127.255(12)			Expt.	2003	Träbert <i>et al.</i> [66]
$Z = 82$						
208.073(53)	244.942(52)	2584.793(51)	2687.576(51)	Th.	2024	This work
207.756	244.734	2584.54	2687.59	Th.	2008	Cheng <i>et al.</i> [46]
	244.845		2687.43	Th.	1997	Chen and Cheng [36]
$Z = 83$						
212.956(59)	250.188(58)	2728.852(57)	2833.347(57)	Th.	2024	This work
213(11)	250(11)	2729(11)	2834(11)	Th.	2019	Kaygorodov <i>et al.</i> [54]
212.599	249.943	2728.56	2833.32	Th.	2008	Cheng <i>et al.</i> [46]
	248.03	2727	2832	Th.	2000	Safronova [39]
			2833.04	Th.	1998	Santos <i>et al.</i> [37]
212.953	250.242	2728.459	2833.154	Th.	1996	Safronova <i>et al.</i> [35]
$Z = 90$						
248.00(14)	287.38(14)	3951.40(13)	4068.64(13)	Th.	2024	This work
248(12)	288(12)	3952(12)	4069(12)	Th.	2019	Kaygorodov <i>et al.</i> [54]
247.461	286.968	3950.97	4068.47	Th.	2008	Cheng <i>et al.</i> [46]
			4068.54	Th.	2000	Cheng <i>et al.</i> [38]
	284.30	3950	4068	Th.	2000	Safronova [39]
			4068.21	Th.	1998	Santos <i>et al.</i> [37]
	287.150		4068.19	Th.	1997	Chen and Cheng [36]
248.072	287.511	3950.874	4068.360	Th.	1996	Safronova <i>et al.</i> [35]
			4068.47(16)	Expt.	1995	Beiersdorfer <i>et al.</i> [63]
$Z = 92$						
258.07(11)	297.91(11)	4380.63(10)	4501.77(10)	Th.	2024	This work
259(13)	299(13)	4382(13)	4503(13)	Th.	2019	Kaygorodov <i>et al.</i> [54]
257.564	297.537	4380.27	4501.66	Th.	2008	Cheng <i>et al.</i> [46]
			4501.73	Th.	2000	Cheng <i>et al.</i> [38]
	294.45	4380	4500	Th.	2000	Safronova [39]
			4501.54	Th.	1998	Santos <i>et al.</i> [37]
	297.744		4501.36	Th.	1997	Chen and Cheng [36]
258.276	298.177	4380.198	4501.602	Th.	1996	Safronova <i>et al.</i> [35]
			4501.59(21)	Expt.	2024	Loetzsch <i>et al.</i> [27]
	297.799(12)			Expt.	2005	Beiersdorfer <i>et al.</i> [22]
			4501.72(27)	Expt.	1993	Beiersdorfer <i>et al.</i> [62]

† Semiempirical prediction.

‡ Compilation of energy levels obtained by fitting to available lines.

Our theoretical predictions for the excitation energies of the $2s2p^3P_{0,1,2}$ and $2s2p^1P_1$ states from the $2s2s^1S_0$ ground state and for the $2s2p^3P_1 \rightarrow 2s2p^3P_0$ and $2s2p^3P_2 \rightarrow 2s2p^3P_1$ transition energies are com-

piled in Tables III and IV, respectively. As the final results, we use the values obtained for the LDF potential and for the maximal sizes of the model subspaces indicated in Sec. II. The uncertainties of the theoretical predictions are estimated according to the procedure summarized in Table II.

Tables III and IV give a detailed comparison of the excitation and transition energies with the previous relativistic calculations and available measurements. We note that for the $2s2p^3P_2 \rightarrow 2s2p^3P_1$ transition in Be-like argon the experimental wavelengths in air are usually reported in literature. The conversion between the air and vacuum wavelengths is accomplished using the three-term formula for the refractive index of air, which is given in Eq. (3) in Ref. [103]. The same approach was

employed, e.g., in Ref. [69]. As can be seen, the previous theoretical studies of Be-like HCIs indeed exhibit a considerable scatter of the results. In general, all these values are in agreement with our predictions. When the uncertainties are specified [48, 50, 54], they are, in principle, consistent. However, our results are much more precise. In Ref. [54], we evaluated the energies of Be-like HCIs in the framework of the CI method, taking into account the nuclear-recoil and QED effect by means of the mass-shift [83, 84, 88] and model-QED [92, 93] operators. The uncertainties in that study have been estimated in a rather conservative manner. A comparison with the present work shows that the accuracy of the approach used in Ref. [54] is at least one order of magnitude higher.

TABLE IV: The $2s2p^3P_1 \rightarrow 2s2p^3P_0$ and $2s2p^3P_2 \rightarrow 2s2p^3P_1$ transition energies in Be-like ions (in eV). The theoretical (Th.) results are compared with the experimental (Expt.) values.

$2s2p^3P_1$ $-2s2p^3P_0$	$2s2p^3P_2$ $-2s2p^3P_1$	Th./Expt.	Year	Reference
$Z = 18$				
0.89024(39)	2.08527(43)	Th.	2024	This work
0.890(95)	2.087(95)	Th.	2019	Kaygorodov <i>et al.</i> [54]
0.888(20)	2.086(20)	Th.	2015	Yerokhin <i>et al.</i> [50]
	2.0859(11)	Th.	2006	Soria Orts <i>et al.</i> [44]
0.8912	2.0866	Th.	2005	Gu [43]
	2.0839	Th.	2003	Draganić <i>et al.</i> [42]
0.8902	2.0807	Th.	2001	Dong <i>et al.</i> [41]
0.8908	2.0871	Th.	1996	Safronova <i>et al.</i> [35]
	2.0854	Th. [†]	1983	Edlén [31]
	2.085339(7)	Expt.	2007	Katai <i>et al.</i> [68]
	2.0853362(7)	Expt.	2006	Soria Orts <i>et al.</i> [44]
	2.0853358(18)	Expt.	2003	Draganić <i>et al.</i> [42]
	2.085388(14)	Expt.	1997	Bieber <i>et al.</i> [64]
$Z = 36$				
10.3556(18)	52.6710(19)	Th.	2024	This work
10.34(73)	52.71(73)	Th.	2019	Kaygorodov <i>et al.</i> [54]
10.392(31)		Th.	2013	Sampaio <i>et al.</i> [48]
10.4341		Th.	2011	Winters <i>et al.</i> [47]
10.3639	52.669	Th.	2008	Cheng <i>et al.</i> [46]
10.3677	52.7083	Th.	2005	Gu [43]
10.3553	52.6658	Th.	1996	Safronova <i>et al.</i> [35]
10.535		Th.	1993	Marques <i>et al.</i> [33]
	52.7449	Th. [†]	1983	Edlén [31]
10.33(26)	52.82(32)	Expt.	1990	Martin <i>et al.</i> [60]
	52.652(11)	Expt.	1989	Denne <i>et al.</i> [58]
$Z = 42$				
14.7174(29)	107.9815(31)	Th.	2024	This work
14.7(12)	108.0(12)	Th.	2019	Kaygorodov <i>et al.</i> [54]
14.7329	107.977	Th.	2008	Cheng <i>et al.</i> [46]
14.7371	108.0691	Th.	2005	Gu [43]
14.7204	107.9659	Th.	1996	Safronova <i>et al.</i> [35]

TABLE IV: Transition energies (*continued*).

$2s2p^3P_1$ $-2s2p^3P_0$	$2s2p^3P_2$ $-2s2p^3P_1$	Th./Expt.	Year	Reference
$Z = 54$				
22.7693(63)	342.1835(73)	Th.	2024	This work
22.8(25)	342.3(25)	Th.	2019	Kaygorodov <i>et al.</i> [54]
22.807	342.167	Th.	2008	Cheng <i>et al.</i> [46]
22.812	342.529	Th.	2005	Gu [43]
22.785	342.119	Th.	1996	Safronova <i>et al.</i> [35]
23.191		Th.	1993	Marques <i>et al.</i> [33]
$Z = 82$				
36.869(26)	2339.851(35)	Th.	2024	This work
36.978	2339.81	Th.	2008	Cheng <i>et al.</i> [46]
37.419		Th.	1993	Marques <i>et al.</i> [33]
$Z = 83$				
37.232(27)	2478.664(36)	Th.	2024	This work
37(11)	2479(11)	Th.	2019	Kaygorodov <i>et al.</i> [54]
37.344	2478.62	Th.	2008	Cheng <i>et al.</i> [46]
37.289	2478.217	Th.	1996	Safronova <i>et al.</i> [35]
$Z = 90$				
39.379(37)	3664.020(52)	Th.	2024	This work
39(12)	3663(12)	Th.	2019	Kaygorodov <i>et al.</i> [54]
39.507	3664.00	Th.	2008	Cheng <i>et al.</i> [46]
39.439	3663.363	Th.	1996	Safronova <i>et al.</i> [35]
$Z = 92$				
39.841(41)	4082.725(56)	Th.	2024	This work
40(13)	4083(13)	Th.	2019	Kaygorodov <i>et al.</i> [54]
39.973	4082.73	Th.	2008	Cheng <i>et al.</i> [46]
39.901	4082.021	Th.	1996	Safronova <i>et al.</i> [35]
	4081.72(27)	Expt.	1998	Beiersdorfer <i>et al.</i> [65]

[†] Semiempirical prediction.

As for the comparison with experimental results, based on Tables III and IV, we may conclude that our theoretical predictions are in good agreement with the most of them, including the ultraprecise measurements of the $2s2p^3P_2 \rightarrow 2s2p^3P_1$ transition in Be-like argon [42, 44]. A discrepancy with the most precise experimental value for the $2s2s^1S_0 \rightarrow 2s2p^3P_1$ excitation energy in Be-like xenon [66], previously noted in Ref. [25], still remains. We emphasize, however, that in this case our theoretical prediction agrees with the more recent experiment [70]. We also note that the measurement of the $2s2p^3P_2 \rightarrow 2s2p^3P_1$ transition energy in Be-like uranium deviates from our result by almost 4 times the experimental uncertainty, while, according to the analysis in Table II, the theoretical accuracy in this case turns out to be almost 5 times higher than the experimental one. The reason for this discrepancy is unclear to us.

Finally, in Table V we show a separation of the ob-

tained theoretical predictions for the excitation and transition energies into the non-QED and QED parts. The former is obtained by diagonalizing the matrix of the effective Hamiltonian H_{eff} , which along with the results of the CI calculations includes only the frequency-dependent correction of the one-photon-exchange contribution (the first diagram in Fig. 1), the non-QED part of the nuclear recoil effect, and the nuclear polarization correction. The QED part covers the remainder, and it is obtained as the difference of the total and non-QED terms. The separation is given based on the calculations for the LDF potential. We hope that the data presented in Tables III, IV, and V as well as the discrepancies with the available experimental data mentioned above will serve as a trigger for new experiments with Be-like HCl, especially in view of the prospects of these systems for rigorous tests of bound-state-QED methods.

TABLE V: Non-QED and QED contributions to the excitation and transition energies in Be-like highly-charged ions (in eV). See the text for details.

Contribution	$2s2p^3P_0$ $-2s2s^1S_0$	$2s2p^3P_1$ $-2s2s^1S_0$	$2s2p^3P_2$ $-2s2s^1S_0$	$2s2p^1P_1$ $-2s2s^1S_0$	$2s2p^3P_1$ $-2s2p^3P_0$	$2s2p^3P_2$ $-2s2p^3P_1$
$Z = 18$						
$E_{\text{non-QED}}$	28.46821	29.35659	31.43689	56.18347	0.88838	2.08030
E_{QED}	-0.11418	-0.11232	-0.10736	-0.11548	0.00185	0.00497
E_{total}	28.35403(41)	29.24427(59)	31.32954(39)	56.06799(70)	0.89024(39)	2.08527(43)
$Z = 36$						
$E_{\text{non-QED}}$	64.0523	74.4028	126.9509	171.7563	10.3504	52.5481
E_{QED}	-1.4217	-1.4166	-1.2937	-1.3363	0.0052	0.1229
E_{total}	62.6306(21)	72.9862(20)	125.6572(19)	170.4200(21)	10.3556(18)	52.6710(19)
$Z = 42$						
$E_{\text{non-QED}}$	77.7434	92.4616	200.2050	250.7716	14.7182	107.7434
E_{QED}	-2.4558	-2.4567	-2.2186	-2.2726	-0.0008	0.2380
E_{total}	75.2876(32)	90.0049(32)	197.9864(29)	248.4990(30)	14.7174(29)	107.9815(31)
$Z = 54$						
$E_{\text{non-QED}}$	110.4804	133.2705	474.8108	538.2090	22.7901	341.5402
E_{QED}	-5.9500	-5.9708	-5.3276	-5.4082	-0.0208	0.6433
E_{total}	104.5305(74)	127.2997(73)	469.4832(70)	532.8009(69)	22.7693(63)	342.1835(73)
$Z = 82$						
$E_{\text{non-QED}}$	234.426	271.385	2608.929	2711.899	36.959	2337.544
E_{QED}	-26.353	-26.443	-24.136	-24.323	-0.090	2.307
E_{total}	208.073(53)	244.942(52)	2584.793(51)	2687.576(51)	36.869(26)	2339.851(35)
$Z = 83$						
$E_{\text{non-QED}}$	240.497	277.823	2754.137	2858.825	37.326	2476.314
E_{QED}	-27.541	-27.635	-25.285	-25.478	-0.093	2.349
E_{total}	212.956(59)	250.188(58)	2728.852(57)	2833.347(57)	37.232(27)	2478.664(36)
$Z = 90$						
$E_{\text{non-QED}}$	285.02	324.52	3986.12	4103.58	39.493	3661.599
E_{QED}	-37.02	-37.14	-34.72	-34.95	-0.114	2.421
E_{total}	248.00(14)	287.38(14)	3951.40(13)	4068.64(13)	39.379(37)	3664.020(52)
$Z = 92$						
$E_{\text{non-QED}}$	298.20	338.16	4418.55	4539.93	39.961	4080.390
E_{QED}	-40.13	-40.25	-37.92	-38.16	-0.120	2.334
E_{total}	258.07(11)	297.91(11)	4380.63(10)	4501.77(10)	39.841(41)	4082.725(56)

IV. SUMMARY

In the present work, the *ab initio* QED approach has been applied to calculate the energies of the $n = 2$ singly excited states in selected Be-like ions in a wide range of nuclear charge numbers: $18 \leq Z \leq 92$. The $2s2s^1S_0$ ground state, with respect to which the excited-state energies are determined, is treated together with the close states of the same symmetry within the QED perturbation theory for quasidegenerate levels. This is done in order to properly describe the impact of the proximity of the levels and their mixing due to

the electron-electron correlations on the QED effects. A similar approach is used to study the pair of the $2s2p^3P_1$ and $2s2p^1P_1$ states. The remaining excited states, $2s2p^3P_0$ and $2s2p^3P_2$, are considered utilizing the standard QED perturbation theory for a single level. The employed approach rigorously takes into account all the first- and second-order QED contributions in the framework of the Furry picture. The third- and higher-order interelectronic-interaction effects are evaluated within the Breit approximation. The model-QED-operator approach is used to estimate the higher-order screened QED effects. In addition, the nuclear-recoil

and nuclear-polarization effects are considered. The calculations are supplemented by a diligent analysis of all possible sources of uncertainties. As a result, the most accurate theoretical predictions for the low-lying excited states have been obtained. In general, perfect agreement is found with the results of high-precision measurements. The calculations performed may serve as a benchmark for the future theoretical and experimental

studies of Be-like highly-charged ions.

ACKNOWLEDGMENTS

The work was supported by the Russian Science Foundation (Grant No. 22-62-00004, <https://rscf.ru/project/22-62-00004/>).

-
- [1] H. F. Beyer and V. P. Shevelko, *Introduction to the Physics of Highly Charged Ions*, Institute of Physics Publishing, Bristol and Philadelphia, 2003.
- [2] J. Sapirstein and K. T. Cheng, Tests of quantum electrodynamics with EBIT, *Can. J. Phys.* **86**, 25 (2008).
- [3] P. Beiersdorfer, Testing QED and atomic-nuclear interactions with high- Z ions, *J. Phys. B: At. Mol. Opt. Phys.* **43**, 074032 (2010).
- [4] D. A. Glazov, Y. S. Kozhedub, A. V. Maiorova, V. M. Shabaev, I. I. Tupitsyn, A. V. Volotka, C. Kozhuharov, G. Plunien, and Th. Stöhlker, Tests of fundamental theories with heavy ions at low-energy regime, *Hyp. Interact.* **199**, 71 (2011).
- [5] A. V. Volotka, D. A. Glazov, O. V. Andreev, V. M. Shabaev, I. I. Tupitsyn, and G. Plunien, Test of many-electron QED effects in the hyperfine splitting of heavy high- Z ions, *Phys. Rev. Lett.* **108**, 073001 (2012).
- [6] V. M. Shabaev, D. A. Glazov, G. Plunien, and A. V. Volotka, Theory of bound-electron g factor in highly charged ions, *J. Phys. Chem. Ref. Data* **44**, 031205 (2015).
- [7] V. M. Shabaev, A. I. Bondarev, D. A. Glazov, M. Y. Kaygorodov, Y. S. Kozhedub, I. A. Maltsev, A. V. Malyshev, R. V. Popov, I. I. Tupitsyn, and N. A. Zubova, Stringent tests of QED using highly charged ions, *Hyp. Interact.* **239**, 60 (2018).
- [8] M. G. Kozlov, M. S. Safronova, J. R. Crespo López-Urrutia, and P. O. Schmidt, Highly charged ions: Optical clocks and applications in fundamental physics, *Rev. Mod. Phys.* **90**, 045005 (2018).
- [9] P. Indelicato, QED tests with highly charged ions, *J. Phys. B: At. Mol. Opt. Phys.* **52**, 232001 (2019).
- [10] V. M. Shabaev, Quantum electrodynamics effects in atoms and molecules, in *Comprehensive Computational Chemistry (First Edition)*, edited by M. Yáñez and R. J. Boyd, pp. 94–128, Elsevier, Oxford, 2024.
- [11] S. Sturm, F. Köhler, J. Zatorski, A. Wagner, Z. Harman, G. Werth, W. Quint, C. H. Keitel, and K. Blaum, High-precision measurement of the atomic mass of the electron, *Nature* **506**, 467 (2014).
- [12] V. M. Shabaev, D. A. Glazov, N. S. Oreshkina, A. V. Volotka, G. Plunien, H.-J. Kluge, and W. Quint, g -factor of heavy ions: A new access to the fine structure constant, *Phys. Rev. Lett.* **96**, 253002 (2006).
- [13] A. V. Volotka and G. Plunien, Nuclear polarization study: New frontiers for tests of QED in heavy highly charged ions, *Phys. Rev. Lett.* **113**, 023002 (2014).
- [14] V. A. Yerokhin, E. Berseneva, Z. Harman, I. I. Tupitsyn, and C. H. Keitel, g factor of light ions for an improved determination of the fine-structure constant, *Phys. Rev. Lett.* **116**, 100801 (2016).
- [15] O. Yu. Andreev, L. N. Labzowsky, G. Plunien, and G. Soff, Testing the time dependence of fundamental constants in the spectra of multicharged ions, *Phys. Rev. Lett.* **94**, 243002 (2005).
- [16] J. C. Berengut, V. A. Dzuba, and V. V. Flambaum, Enhanced laboratory sensitivity to variation of the fine-structure constant using highly charged ions, *Phys. Rev. Lett.* **105**, 120801 (2010).
- [17] N. S. Oreshkina, S. M. Cavaletto, N. Michel, Z. Harman, and C. H. Keitel, Hyperfine splitting in simple ions for the search of the variation of fundamental constants, *Phys. Rev. A* **96**, 030501 (2017).
- [18] V. M. Shabaev, D. A. Glazov, A. M. Ryzhkov, C. Brandau, G. Plunien, W. Quint, A. M. Volchkova, and D. V. Zinenko, Ground-state g factor of highly charged ^{229}Th ions: An access to the M1 transition probability between the isomeric and ground nuclear states, *Phys. Rev. Lett.* **128**, 043001 (2022).
- [19] S. A. King, L. J. Spieß, P. Micke, A. Wilzewski, T. Leopold, E. Benkler, R. Lange, N. Huntemann, A. Surzhykov, V. A. Yerokhin, J. R. Crespo López-Urrutia, and P. O. Schmidt, An optical atomic clock based on a highly charged ion, *Nature* **611**, 43 (2022).
- [20] J. Schweppe, A. Belkacem, L. Blumenfeld, N. Claytor, B. Feinberg, H. Gould, V. E. Kostroun, L. Levy, S. Misawa, J. R. Mowat, and M. H. Prior, Measurement of the Lamb shift in lithiumlike uranium (U^{89+}), *Phys. Rev. Lett.* **66**, 1434 (1991).
- [21] C. Brandau, C. Kozhuharov, A. Müller, W. Shi, S. Schippers, T. Bartsch, S. Böhm, C. Böhme, A. Hofknecht, H. Knopp, N. Grün, W. Scheid, T. Steih, F. Bosch, B. Franzke, P. H. Mokler, F. Nolden, M. Steck, T. Stöhlker, and Z. Stachura, Precise determination of the $2s_{1/2}-2p_{1/2}$ splitting in very heavy lithiumlike ions utilizing dielectronic recombination, *Phys. Rev. Lett.* **91**, 073202 (2003).
- [22] P. Beiersdorfer, H. Chen, D. B. Thorn, and E. Träbert, Measurement of the two-loop Lamb shift in lithiumlike U^{89+} , *Phys. Rev. Lett.* **95**, 233003 (2005).
- [23] Y. S. Kozhedub, O. V. Andreev, V. M. Shabaev, I. I. Tupitsyn, C. Brandau, C. Kozhuharov, G. Plunien, and T. Stöhlker, Nuclear deformation effect on the binding energies in heavy ions, *Phys. Rev. A* **77**, 032501 (2008).
- [24] J. Sapirstein and K. T. Cheng, S -matrix calculations of energy levels of the lithium isoelectronic sequence, *Phys. Rev. A* **83**, 012504 (2011).
- [25] A. V. Malyshev, D. A. Glazov, Y. S. Kozhedub, I. S. Anisimova, M. Y. Kaygorodov, V. M. Shabaev, and I. I. Tupitsyn, *Ab initio* calculations of energy levels in Be-like xenon: Strong interference between electron-correlation and QED effects, *Phys. Rev. Lett.*

- 126, 183001 (2021).
- [26] A. V. Malyshev, Y. S. Kozhedub, and V. M. Shabaev, *Ab initio* calculations of the $2p_{3/2} \rightarrow 2s$ transition in He-, Li-, and Be-like uranium, *Phys. Rev. A* **107**, 042806 (2023).
- [27] R. Loetzsch, H. F. Beyer, L. Duval, U. Spillmann, D. Banaś, P. Dergham, F. M. Kröger, J. Glorius, R. E. Grisenti, M. Guerra, A. Gumberidze, R. Heß, P.-M. Hillenbrand, P. Indelicato, P. Jagodzinski, E. Lamour, B. Lorentz, S. Litvinov, Y. A. Litvinov, J. Machado, N. Paul, G. G. Paulus, N. Petridis, J. P. Santos, M. Scheidel, R. S. Sidhu, M. Steck, S. Steydli, K. Szary, S. Trotsenko, I. Uschmann, G. Weber, Th. Stöhlker, and M. Trassinelli, Testing quantum electrodynamics in extreme fields using helium-like uranium, *Nature* **625**, 673 (2024).
- [28] L. Armstrong, W. R. Fielder, and D. L. Lin, Relativistic effects on transition probabilities in the Li and Be isoelectronic sequences, *Phys. Rev. A* **14**, 1114 (1976).
- [29] M. A. Braun, A. D. Gurchumelia, and U. I. Safronova, *Relativistic Theory of Atom*, Nauka, Moscow, 1984.
- [30] K. T. Cheng, Y. K. Kim, and J. P. Desclaux, Electric dipole, quadrupole, and magnetic dipole transition probabilities of ions isoelectronic to the first-row atoms, Li through F, *At. Data Nucl. Data Tables* **24**, 111 (1979).
- [31] B. Edlén, Comparison of theoretical and experimental level values of the $n = 2$ complex in ions isoelectronic with Li, Be, O and F, *Phys. Scr.* **28**, 51 (1983).
- [32] E. Lindroth and J. Hvarfner, Relativistic calculation of the $2^1S_0 - 2^1,3P_1$ transitions in berylliumlike molybdenum and berylliumlike iron, *Phys. Rev. A* **45**, 2771 (1992).
- [33] J. P. Marques, F. Parente, and P. Indelicato, Hyperfine quenching of the $1s^2 2s 2p^3 P_0$ level in berylliumlike ions, *Phys. Rev. A* **47**, 929 (1993).
- [34] X.-W. Zhu and K. T. Chung, Energies and fine structures of $1s^2 2snp$ ($n = 2, 3$) $^1P^o$ and $^3P_{2,1,0}^o$ states of Be-like ions, *Phys. Rev. A* **50**, 3818 (1994).
- [35] M. S. Safronova, W. R. Johnson, and U. I. Safronova, Relativistic many-body calculations of the energies of $n = 2$ states for the berylliumlike isoelectronic sequence, *Phys. Rev. A* **53**, 4036 (1996).
- [36] M. H. Chen and K. T. Cheng, Energy levels of the ground state and the $2s2p$ ($J = 1$) excited states of berylliumlike ions: A large-scale, relativistic configuration-interaction calculation, *Phys. Rev. A* **55**, 166 (1997).
- [37] J. Santos, J. Marques, F. Parente, E. Lindroth, S. Boucard, and P. Indelicato, Multiconfiguration Dirac-Fock calculation of transition energies in highly ionized bismuth, thorium, and uranium, *Eur. Phys. J. D* **1**, 149 (1998).
- [38] K. T. Cheng, M. H. Chen, and J. Sapirstein, Quantum electrodynamic corrections in high- Z Li-like and Be-like ions, *Phys. Rev. A* **62**, 054501 (2000).
- [39] U. I. Safronova, Excitation energies and transition rates in Be-, Mg-, and Zn-like ions, *Mol. Phys.* **98**, 1213 (2000).
- [40] S. Majumder and B. P. Das, Relativistic magnetic quadrupole transitions in Be-like ions, *Phys. Rev. A* **62**, 042508 (2000).
- [41] C. Z. Dong, S. Fritzsche, B. Fricke, and W.-D. Sepp, Ab-initio calculations for forbidden M1 transitions in Ar^{13+} and Ar^{14+} ions, *Phys. Scr.* **2001**, 294 (2001).
- [42] I. Draganić, J. R. Crespo López-Urrutia, R. DuBois, S. Fritzsche, V. M. Shabaev, R. Soria Orts, I. I. Tupitsyn, Y. Zou, and J. Ullrich, High precision wavelength measurements of QED-sensitive forbidden transitions in highly charged argon ions, *Phys. Rev. Lett.* **91**, 183001 (2003).
- [43] M. F. Gu, Energies of $1s^2 2l^q$ ($1 \leq q \leq 8$) states for $Z \leq 60$ with a combined configuration interaction and many-body perturbation theory approach, *At. Data Nucl. Data Tables* **89**, 267 (2005).
- [44] R. Soria Orts, Z. Harman, J. R. Crespo López-Urrutia, A. N. Artemyev, H. Bruhns, A. J. G. Martínez, U. D. Jentschura, C. H. Keitel, A. Lapierre, V. Mironov, V. M. Shabaev, H. Tawara, I. I. Tupitsyn, J. Ullrich, and A. V. Volotka, Exploring relativistic many-body recoil effects in highly charged ions, *Phys. Rev. Lett.* **97**, 103002 (2006).
- [45] H. C. Ho, W. R. Johnson, S. A. Blundell, and M. S. Safronova, Third-order many-body perturbation theory calculations for the beryllium and magnesium isoelectronic sequences, *Phys. Rev. A* **74**, 022510 (2006).
- [46] K. T. Cheng, M. H. Chen, and W. R. Johnson, Hyperfine quenching of the $2s2p^3 P_0$ state of berylliumlike ions, *Phys. Rev. A* **77**, 052504 (2008).
- [47] D. F. A. Winters, T. Kühl, D. H. Schneider, P. Indelicato, R. Reuschl, R. Schuch, E. Lindroth, and T. Stöhlker, Laser spectroscopy of the $(1s^2 2s 2p)^3 P_0 - ^3 P_1$ level splitting in Be-like krypton, *Phys. Scr.* **2011**, 014013 (2011).
- [48] J. M. Sampaio, F. Parente, C. Nazé, M. Godefroid, P. Indelicato, and J. P. Marques, Relativistic calculations of $1s^2 2s 2p$ level splitting in Be-like Kr, *Phys. Scr.* **T156**, 014015 (2013).
- [49] V. A. Yerokhin, A. Surzhykov, and S. Fritzsche, Relativistic configuration-interaction calculation of $K\alpha$ transition energies in berylliumlike iron, *Phys. Rev. A* **90**, 022509 (2014).
- [50] V. A. Yerokhin, A. Surzhykov, and S. Fritzsche, Relativistic configuration-interaction calculation of $K\alpha$ transition energies in beryllium-like argon, *Phys. Scr.* **90**, 054003 (2015).
- [51] K. Wang, X. L. Guo, H. T. Liu, D. F. Li, F. Y. Long, X. Y. Han, B. Duan, J. G. Li, M. Huang, Y. S. Wang, R. Hutton, Y. M. Zou, J. L. Zeng, C. Y. Chen, and J. Yan, Systematic calculations of energy levels and transition rates of Be-like ions with $Z = 10 - 30$ using a combined configuration interaction and many-body perturbation theory approach, *Astrophys. J. Suppl. Ser.* **218**, 16 (2015).
- [52] A. A. El-Maaref, S. Schippers, and A. Müller, Ab-initio calculations of level energies, oscillator strengths and radiative rates for E1 transitions in beryllium-like iron, *Atoms* **3**, 2 (2015).
- [53] K. K. Li, L. Zhuo, C. M. Zhang, C. Chen, and B. C. Gou, Energies and hyperfine structures of the $1s^2 2s 2p^3 P^o$ state of Be-like ions with $Z = 11 - 18$, *Can. J. Phys.* **95**, 720 (2017).
- [54] M. Y. Kaygorodov, Y. S. Kozhedub, I. I. Tupitsyn, A. V. Malyshev, D. A. Glazov, G. Plunien, and V. M. Shabaev, Relativistic calculations of the ground and inner- L -shell excited energy levels of berylliumlike ions, *Phys. Rev. A* **99**, 032505 (2019).

- [55] A. V. Malyshev, Y. S. Kozhedub, I. S. Anisimova, D. A. Glazov, M. Y. Kaygorodov, I. I. Tupitsyn, and V. M. Shabaev, Binding energy of the ground state of beryllium-like molybdenum: Correlation and quantum-electrodynamical effects, *Opt. Spectrosc.* **129**, 652 (2021).
- [56] K. G. Widing, Fe XXIII 263 Å and Fe XXIV 255 Å emission in solar flares, *Astrophys. J.* **197**, L33 (1975).
- [57] K. P. Dere, Spectral lines observed in solar flares between 171 and 630 angstroms, *Astrophys. J.* **221**, 1062 (1978).
- [58] B. Denne, E. Hinnov, J. Ramette, and B. Saoutic, Spectrum lines of Kr XXVIII – Kr XXXIV observed in the JET tokamak, *Phys. Rev. A* **40**, 1488 (1989).
- [59] B. Denne, G. Magyar, and J. Jacquinet, Berylliumlike Mo XXXIX and lithiumlike Mo XL observed in the Joint European Torus tokamak, *Phys. Rev. A* **40**, 3702 (1989).
- [60] S. Martin, A. Denis, M. C. Buchet-Poulizac, J. P. Buchet, and J. Désesquelles, $2s - 2p$ transitions in heliumlike and lithiumlike krypton, *Phys. Rev. A* **42**, 6570 (1990).
- [61] J. Sugar and A. Musgrove, Energy levels of krypton, Kr I through Kr XXXVI, *J. Phys. Chem. Ref. Data* **20**, 859 (1991).
- [62] P. Beiersdorfer, D. Knapp, R. E. Marrs, S. R. Elliott, and M. H. Chen, Structure and Lamb shift of $2s_{1/2} - 2p_{3/2}$ levels in lithiumlike U^{89+} through neonlike U^{82+} , *Phys. Rev. Lett.* **71**, 3939 (1993).
- [63] P. Beiersdorfer, A. Osterheld, S. R. Elliott, M. H. Chen, D. Knapp, and K. Reed, Structure and Lamb shift of $2s_{1/2} - 2p_{3/2}$ levels in lithiumlike Th^{87+} through neonlike Th^{80+} , *Phys. Rev. A* **52**, 2693 (1995).
- [64] D. J. Bieber, H. S. Margolis, P. K. Oxley, and J. D. Silver, Studies of magnetic dipole transitions in highly charged argon and barium using an electron beam ion trap, *Phys. Scr.* **T73**, 64 (1997).
- [65] P. Beiersdorfer, A. L. Osterheld, and S. R. Elliott, Measurements and modeling of electric-dipole-forbidden $2p_{1/2} - 2p_{3/2}$ transitions in fluorinelike U^{81+} through berylliumlike U^{88+} , *Phys. Rev. A* **58**, 1944 (1998).
- [66] E. Träbert, P. Beiersdorfer, J. K. Lepson, and H. Chen, Extreme ultraviolet spectra of highly charged Xe ions, *Phys. Rev. A* **68**, 042501 (2003).
- [67] D. Feili, B. Zimmermann, C. Neacsu, Ph. Bosselmann, K.-H. Schartner, F. Folkmann, A. E. Livingston, E. Träbert, and P. H. Mokler, $2s^2\ ^1S_0 - 2s2p\ ^3P_1$ intercombination transition wavelengths in Be-like Ag^{43+} , Sn^{46+} , and Xe^{50+} ions, *Phys. Scr.* **71**, 48 (2005).
- [68] R. Katai, S. Morita, and M. Goto, Identification and intensity analysis on forbidden magnetic dipole emission lines of highly charged Al, Ar, Ti and Fe ions in LHD, *J. Quant. Spectrosc. Radiat. Transf.* **107**, 120 (2007).
- [69] E. B. Saloman, Energy levels and observed spectral lines of ionized argon, ArII through ArXVIII, *J. Phys. Chem. Ref. Data* **39**, 033101 (2010).
- [70] D. Bernhardt, C. Brandau, Z. Harman, C. Kozhuharov, S. Böhm, F. Bosch, S. Fritzsche, J. Jacobi, S. Kieslich, H. Knopp, F. Nolden, W. Shi, Z. Stachura, M. Steck, Th. Stöhlker, S. Schippers, and A. Müller, Spectroscopy of berylliumlike xenon ions using dielectronic recombination, *J. Phys. B: At. Mol. Opt. Phys.* **48**, 144008 (2015).
- [71] W. H. Furry, On bound states and scattering in positron theory, *Phys. Rev.* **81**, 115 (1951).
- [72] V. M. Shabaev, Two-time Green's function method in quantum electrodynamics of high- Z few-electron atoms, *Phys. Rep.* **356**, 119 (2002).
- [73] V. M. Shabaev, I. I. Tupitsyn, K. Pachucki, G. Plunien, and V. A. Yerokhin, Radiative and correlation effects on the parity-nonconserving transition amplitude in heavy alkali-metal atoms, *Phys. Rev. A* **72**, 062105 (2005).
- [74] V. A. Yerokhin and V. M. Shabaev, Lamb shift of $n = 1$ and $n = 2$ states of hydrogen-like atoms, $1 \leq Z \leq 110$, *J. Phys. Chem. Ref. Data* **44**, 033103 (2015).
- [75] V. A. Yerokhin, Two-loop self-energy in the Lamb shift of the ground and excited states of hydrogenlike ions, *Phys. Rev. A* **97**, 052509 (2018).
- [76] A. V. Malyshev, A. V. Volotka, D. A. Glazov, I. I. Tupitsyn, V. M. Shabaev, and G. Plunien, QED calculation of the ground-state energy of berylliumlike ions, *Phys. Rev. A* **90**, 062517 (2014).
- [77] A. V. Malyshev, D. A. Glazov, A. V. Volotka, I. I. Tupitsyn, V. M. Shabaev, G. Plunien, and Th. Stöhlker, Ground-state ionization energies of boronlike ions, *Phys. Rev. A* **96**, 022512 (2017).
- [78] Y. S. Kozhedub, A. V. Malyshev, D. A. Glazov, V. M. Shabaev, and I. I. Tupitsyn, QED calculation of electron-electron correlation effects in heliumlike ions, *Phys. Rev. A* **100**, 062506 (2019).
- [79] A. V. Malyshev, Y. S. Kozhedub, D. A. Glazov, I. I. Tupitsyn, and V. M. Shabaev, QED calculations of the $n = 2$ to $n = 1$ x-ray transition energies in middle- Z heliumlike ions, *Phys. Rev. A* **99**, 010501(R) (2019).
- [80] V. F. Bratzev, G. B. Deyneka, and I. I. Tupitsyn, Application of the Hartree-Fock method to calculation of relativistic atomic wave functions, *Izv. Acad. Nauk SSSR, Ser. Fiz.* **41**, 2655 (1977), [*Bull. Acad. Sci. USSR, Phys. Ser.* **41**, 173 (1977)].
- [81] I. I. Tupitsyn, V. M. Shabaev, J. R. Crespo López-Urrutia, I. Draganić, R. Soria Orts, and J. Ullrich, Relativistic calculations of isotope shifts in highly charged ions, *Phys. Rev. A* **68**, 022511 (2003).
- [82] Y. S. Kozhedub, A. V. Volotka, A. N. Artemyev, D. A. Glazov, G. Plunien, V. M. Shabaev, I. I. Tupitsyn, and Th. Stöhlker, Relativistic recoil, electron-correlation, and QED effects on the $2p_j - 2s$ transition energies in Li-like ions, *Phys. Rev. A* **81**, 042513 (2010).
- [83] V. M. Shabaev, Mass corrections in a strong nuclear field, *Teor. Mat. Fiz.* **63**, 394 (1985), [*Theor. Math. Phys.* **63**, 588 (1985)].
- [84] V. M. Shabaev, Nuclear recoil effect in relativistic theory of multiply charged ions, *Yad. Fiz.* **47**, 107 (1988), [*Sov. J. Nucl. Phys.* **47**, 69 (1988)].
- [85] V. M. Shabaev, QED theory of the nuclear recoil effect in atoms, *Phys. Rev. A* **57**, 59 (1998).
- [86] K. Pachucki and H. Grotch, Pure recoil corrections to hydrogen energy levels, *Phys. Rev. A* **51**, 1854 (1995).
- [87] G. S. Adkins, S. Morrison, and J. Sapirstein, Recoil corrections in highly charged ions, *Phys. Rev. A* **76**, 042508 (2007).
- [88] C. W. P. Palmer, Reformulation of the theory of the mass shift, *J. Phys. B: At. Mol. Phys.* **20**, 5987 (1987).

- [89] K. Pachucki and V. A. Yerokhin, Heavy-particle quantum electrodynamics, *Phys. Rev. A* **110**, 032804 (2024).
- [90] G. Plunien and G. Soff, Nuclear-polarization contribution to the Lamb shift in actinide nuclei, *Phys. Rev. A* **51**, 1119 (1995); **53**, 4614(E) (1996).
- [91] A. V. Nefiodov, L. N. Labzowsky, G. Plunien, and G. Soff, Nuclear polarization effects in spectra of multicharged ions, *Phys. Lett. A* **222**, 227 (1996).
- [92] V. M. Shabaev, I. I. Tupitsyn, and V. A. Yerokhin, Model operator approach to the Lamb shift calculations in relativistic many-electron atoms, *Phys. Rev. A* **88**, 012513 (2013).
- [93] V. M. Shabaev, I. I. Tupitsyn, and V. A. Yerokhin, QEDMOD: Fortran program for calculating the model Lamb-shift operator, *Comput. Phys. Commun.* **189**, 175 (2015); **223**, 69 (2018).
- [94] E. Tiesinga, P. J. Mohr, D. B. Newell, and B. N. Taylor, CODATA recommended values of the fundamental physical constants: 2018, *Rev. Mod. Phys.* **93**, 025010 (2021).
- [95] J. Sapirstein, K. T. Cheng, and M. H. Chen, Potential independence of the solution to the relativistic many-body problem and the role of negative-energy states in heliumlike ions, *Phys. Rev. A* **59**, 259 (1999).
- [96] V. M. Shabaev, Schrodinger-like equation for the relativistic few-electron atom, *J. Phys. B: At. Mol. Opt. Phys.* **26**, 4703 (1993).
- [97] G. W. Drake, Theoretical energies for the $n = 1$ and 2 states of the helium isoelectronic sequence up to $Z = 100$, *Can. J. Phys.* **66**, 586 (1988).
- [98] A. N. Artemyev, V. M. Shabaev, V. A. Yerokhin, G. Plunien, and G. Soff, QED calculation of the $n = 1$ and $n = 2$ energy levels in He-like ions, *Phys. Rev. A* **71**, 062104 (2005).
- [99] V. M. Shabaev, A. N. Artemyev, T. Beier, G. Plunien, V. A. Yerokhin, and G. Soff, Recoil correction to the ground-state energy of hydrogenlike atoms, *Phys. Rev. A* **57**, 4235 (1998).
- [100] I. A. Aleksandrov, A. A. Shchepetnov, D. A. Glazov, and V. M. Shabaev, Finite nuclear size corrections to the recoil effect in hydrogenlike ions, *J. Phys. B: At. Mol. Opt. Phys.* **48**, 144004 (2015).
- [101] I. S. Anisimova, A. V. Malyshev, D. A. Glazov, M. Y. Kaygorodov, Y. S. Kozhedub, G. Plunien, and V. M. Shabaev, Model-QED-operator approach to relativistic calculations of the nuclear recoil effect in many-electron atoms and ions, *Phys. Rev. A* **106**, 062823 (2022).
- [102] K. Pachucki and V. A. Yerokhin, QED theory of the nuclear recoil with finite size, *Phys. Rev. Lett.* **130**, 053002 (2023).
- [103] E. R. Peck and K. Reeder, Dispersion of air*, *J. Opt. Soc. Am.* **62**, 958 (1972).